JCTC Journal of Chemical Theory and Computation

ARTICLE

pubs.acs.org/JCTC

Exploring Anharmonic Nuclear Dynamics and Spectroscopy Using the Kratzer Oscillator

Mohamad Toutounji

Department of Chemistry, College of Science, United Arab Emirates University, Al-Ain, United Arab Emirates

ABSTRACT: The Kratzer oscillator is useful in modeling anharmonic molecular vibrations; therefore, its underlying theory is briefly explored in this study. The linear dipole moment time correlation function, within the Condon approximation, is analytically evaluated, and linear absorption lineshapes are calculated at different temperatures. An important integral formula of Landau and Liftshitz is, for the first time, utilized to evaluate the anharmonic Franck−Condon factor (FCF) resulting from modeling the initial and final states by Kratzer potentials. In addition, an exact closed-form expression of the FCF for the linearly displaced and shape-distorted final state energy curve, with respect to the ground state, is reported. Within the context of Mukamel formalism, nonlinear spectral/temporal lineshapes, such as hole-burning, photon echo, and pump−probe signals, may not be calculated without nonlinear response theory using the so-called "four-point dipole moment time correlation function". The above FCFs will be employed to calculate optical linear and nonlinear spectra at different temperatures utilizing a previously developed formula [Toutounji, M. *J. Phys. Chem. C* **2010**, in press], whereby a hole-burned absorption lineshape may be found using a linear dipole moment time correlation function.

I. INTRODUCTION

Molecular vibrations are more realistically modeled by anharmonic oscillators such as Morse, Kratzer, or Rosen-Morse[1] oscillators, all of which render sound treatment of anharmonic molecules. Recently, the Morse potential has been used for modeling diatomic molecules, or local modes,[2,3] because it has been proven to render qualified results, accounting for important quantum mechanical properties of molecules.[4] While considerable attention has been given to calculating Franck−Condon factors (FCFs) and linear and nonlinear absorption lineshapes of the Morse oscillator,[2,3,5−9] little attention has been devoted to that of Kratzer.[10−12] Various techniques have been employed at different levels of rigor, approximation, and applicability to deal with the Morse oscillator and its consequent dynamics.[13,14]

Although the Morse oscillator has been at the forefront in modeling anharmonic dynamics, utilizing the Kratzer oscillator has not been as common in chemistry[10−12] as has it been in physics[15−17] and mathematics,[18−22] in an effort to solve the corresponding Schrodinger equation using a Laplace transform approach. Recently, the Kratzer oscillator has been drawing some attention in physics; for example, constructing ladder operators and coherent states of the Kratzer oscillator[23] has been established, employing properties of the corresponding eigenfunctions. It has been noted that the Kratzer oscillator has few advantages over that of the Morse oscillator. For example, the latter has a finite number of bound states, whereas the former has an infinite number of them. The Kratzer potential energy curve has been reported, in the works of Van Hooydonk,[12,24−26] to be superior to that of the Morse potential energy curve in fitting the energies of ∼300 diatomic molecules. While the Kratzer oscillator outperforms the Morse oscillator in some molecules, it certainly outperforms harmonic oscillators in all molecules. In addition, a molecular hydrogen (H_2) potential energy curve does not follow the Morse potential: 90%−95% of it comes from that of Kratzer, and the remaining 5%−10% is attributed to quartic potential behavior. An excellent nonmathematical treatment of H_2 and its vibrational levels using Kratzer potential analysis is provided in ref 26. The H_2 experimental vibrational ground-state energy is 2170.08 cm^{-1} and that calculated using the Kratzer ground-state eigenvalue yields 2170.12 cm^{-1}. The roto-vibrational Schrodinger equation with the Kratzer potential can be solved exactly when rotation (repulsive centrifugal potential) is included, which cannot be done with the Morse potential. (This property, in its own right, is a plus for a Kratzer roto-vibrator. The Morse oscillator Schrodinger equation can only be solved exactly if the vibrator is rotationless.) Another motivation for exploring Kratzer oscillator anharmonic dynamics is that its eigenfunctions have been used previously as a basis set for diatomic molecules, rendering sound results.[11] In addition, important matrix elements that were evaluated by Secrest[11] have rendered finite values for *all* rotational states (finite angular momentum), whereas those values are finite *only* for the zero-rotation state in the case of the Morse oscillator. Needless to mention, the Kratzer oscillator eigenfunctions are easier to deal with than those of the Morse oscillator.

In light of the above, the consequent linear and nonlinear lineshapes and spectral dynamics of employing the Kratzer oscillator have not yet been explored. Therefore, carrying out this exploration in this study is deemed necessary and should prove useful in this study. As such, this article is organized as follows. Section II presents the foundations needed for understanding the underlying theory of the Kratzer oscillator. Section III briefly draws the similarities and differences between the Kratzer and Morse oscillators. A methodology is developed in section IV, to account for both vibrational coherences and

Received: December 13, 2010
Published: May 06, 2011

broadening due to pure electronic dephasing. Section V calculates the hole-burning absorption lineshape using the Kratzer oscillator. Results and discussion are provided in section VI. Concluding remarks and prospects are provided in section VII.

II. BACKGROUND ON THE KRATZER OSCILLATOR

While the Morse potential is a three-parameter potential, the Kratzer oscillator is only a two-parameter potential. The parameters of the former are the Kratzer well depth (D_e), the equilibrium internuclear distance (r_e), and the potential width/shape (a; this is often known as the Morse parameter), whereas the latter can only accommodate the bond strength (D_e) and length (r_e). The Kratzer potential assumes this form:

$$V(r) = D_e\left[\left(\frac{r - r_e}{r}\right)^2 - 1\right] \tag{1}$$

where D_e is the well depth and r_e is the equilibrium internuclear distance. A generic shape of the Kratzer potential function is displayed in Figure 1, in which the similarity between the Kratzer potential and that of Morse is readily observed. (The numbers on the abscissa are arbitrary and do not reflect any physicality.) The mth vibrational eigenfunction of the Kratzer oscillator, in coordinate representation, reads as follows:[16]

$$\Psi_m(q) = A_m q^{\lambda} e^{-\eta_m q}\, {}_1F_1\left(\begin{matrix}\lambda - \Omega^2/\eta_m \\ 2\lambda\end{matrix}\middle| 2\eta_m q\right) \tag{2}$$

where ${}_1F_1(\cdot)$ is the confluent hypergeometric function, and the nuclear coordinate q is defined over the range of $0 < q < \infty$. The parameters λ, η_m, and the normalization constant A_m are given by

$$\lambda = \frac{1}{2} + \sqrt{\Omega^2 + \frac{1}{4}} \tag{2a}$$

$$\eta_m{}^2 = \frac{2\mu r_e{}^2(D_e - E_m)}{\hbar^2} \tag{2b}$$

and

$$A_m = \frac{1}{\sqrt{r_e(m + \lambda)}}\sqrt{\frac{\Gamma(2\lambda + m)}{2m!\Gamma^2(2\lambda)}}\left(\frac{2\lambda(\lambda - 1)}{\lambda + m}\right)^{\lambda + (1/2)} \tag{2c}$$

with $\Gamma(\cdot)$ being the Gamma function, $\Omega^2 = 2\mu r_e{}^2 D_e/\hbar^2$, and $q = r/r_e$. E_m in eq 2b are the eigenenergies of the Kratzer oscillator and are given by[16]

$$E_m = D_e\left[1 - \frac{\Omega^2}{(m + \lambda)^2}\right] \qquad m = 0, 1, 2, \ldots \tag{3}$$

This nonstandard integral is needed for evaluating the normalization constant, A_m:

$$\int_0^{\infty} q^{2\lambda} e^{-2\eta_m q}\left[{}_1F_1\left(\begin{matrix}-m \\ 2\lambda\end{matrix}\middle| 2\eta_m q\right)\right]^2 dq = \frac{2(\lambda + m)m!\Gamma(2\lambda)}{(2\eta_m)^{2\lambda + 1}(2\lambda)_m}$$

Kratzer oscillator eigenfunctions are most often reported unnormalized, and, in cases where the normalization constant was reported, it was inaccurate, because it did not yield a value of unity when numerically evaluated; therefore, the above challenging integral had to be evaluated. One can define the *Kratzer coordinate*, analogous to that of the Morse oscillator (*vide infra*),[2] as $z = 2\eta q$; as such,

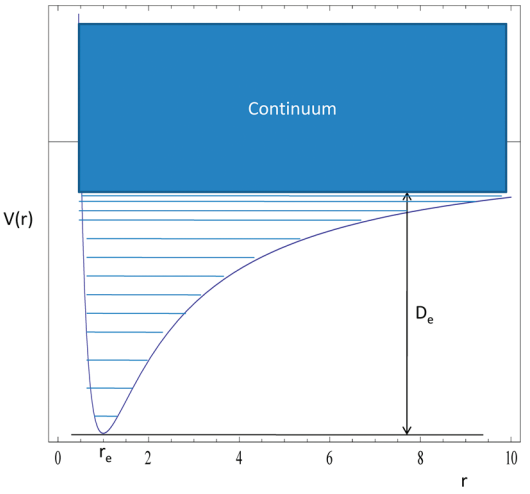

Figure 1. Kratzer potential displaying bound/quantitized and continuum/scattering states. It looks very similar to the Morse potential, which has three parameters—namely, well depth (D_e), width (a), and bond length (r_e)—whereas the Kratzer potential lacks the width parameter a.

$$\Psi_m(z) = A_m(2\eta_m)^{-\lambda} z^{\lambda} e^{-z/2}\, {}_1F_1\left(\begin{matrix}-m \\ 2\lambda\end{matrix}\middle| z\right) \tag{4}$$

An important quantity of the Kratzer oscillator is the dissociation energy (D_0), which is related to the force constant (which can be defined as $k_e = \mu\omega^2$). However, the Kratzer force constant (k_e) is given by[18]

$$k_e = \frac{d^2}{dr^2}V(r)\bigg|_{r_e} = \frac{2D_e}{r_e^2} \tag{5}$$

III. CONNECTION TO THE MORSE OSCILLATOR AND THE HYDROGEN ATOM (COULOMB POTENTIAL)

The Morse oscillator has been explored extensively by different groups.[2−9,14] As noted earlier, one can interestingly observe that the Morse and Kratzer potentials seem to have similar sets of eigenfunctions: both sets are products of a power function, an exponential function, and associated Laguerre polynomials. The vibrational Morse oscillator Hamiltonian for the excited state reads

$$H = \frac{P^2}{2\mu} + D_e\left\{\exp\left[-2a(q - q_0)\right] - \left[2\exp -a(q - q_0)\right]\right\} \tag{6}$$

defined over a range of $-\infty < q < \infty$, with P and q being the momentum and position, respectively. The eigenfunctions of the Morse oscillator are expressed in terms of the generalized Laguerre polynomials:

$$\Phi_n(q) = B_n\left\{2\nu \exp\left[-a(q - q_0)\right]\right\}^s \exp\left\{-\nu \exp\left[-a(q - q_0)\right]\right\} L_n{}^{2s} 2\nu \exp\left[-a(q - q_0)\right] \tag{7}$$

dx.doi.org/10.1021/ct1007185 |J. Chem. Theory Comput. 2011, 7, 1804–1813

where

$$B_n = \sqrt{\frac{a\Gamma(n+1)2s}{\Gamma(2\nu-n)}} \tag{7a}$$

where $\nu \equiv (2\mu D_e)^{1/2}/(\hbar a)$ and $2s = 2\nu - 2n - 1$. One readily observes that the variable y, which is often called the *Morse coordinate* (defined as $y \equiv 2\nu \exp[-a(q-q_0)]$) can serve as an independent variable in eq 7 and the parameter s is directly related to the number of bound states. Hence, the Morse eigenfunctions, expressed in terms of the Morse coordinate, read as

$$\Phi_n(y) = B_n y^s \exp\left(-\frac{y}{2}\right) L_n^{2s}(y) \tag{8}$$

One can employ this relationship,

$$L_i^{\lambda}(x) = \frac{\Gamma(\lambda+i+1)}{i!\Gamma(\lambda+1)} {}_1F_1\left(\begin{matrix}-\mu \\ \lambda+1\end{matrix}\middle| x\right) \tag{9}$$

to express Laguerre polynomials in terms of confluent hypergeometric functions, so that Morse oscillator eigenfunctions can be compared to those of the Kratzer oscillator. Therefore, Morse bound states may be recast as

$$\Phi_n(y) = B_n C_n y^s \exp\left(-\frac{y}{2}\right) {}_1F_1\left(\begin{matrix}-n \\ 2s+1\end{matrix}\middle| y\right) \tag{10}$$

where

$$C_n = \frac{\Gamma(2s+n+1)}{n!\Gamma(n+1)} \tag{10a}$$

As such, casting Morse eigenfunctions in terms of confluent hypergeometric functions, as in eq 10, will help pinpoint the similarities and differences between the two anharmonic oscillators in modeling molecular vibrations. One may readily notice that both the Kratzer and Morse oscillators stationary states $\Psi_m(z)$ and $\Phi_n(y)$ are made of power functions (z^{λ} and y^s), exponential functions ($\exp(-z/2)$ and $\exp(-y/2)$), and confluent hypergeometric functions, both of which are linear in nuclear coordinates.

Other important quantities, such as the potential width parameter a ($a \equiv (k_e^{MO}/2D_e)^{1/2}$, with k_e^{MO} being the force constant at the minimum of the Morse potential, potential depth D_e and anharmonicity constant χ governed by the number of bound states: $\chi = 1/(2\nu)$. (Pollak reported dynamical calculations with two- and five-state Morse oscillators in order to probe vary large anharmonic effects.[4]) While the Kratzer force constant k_e is given in eq 5, that of Morse is $k_e^{MO} = 2aD_e^2$, which will give rise to some spectroscopic and dynamical disparities rendered by both oscillators, as the following discussion will demonstrate.

A fundamental feature of the Kratzer oscillator is that it has an infinite number of vibrational bound states, thereby placing restriction on its anharmonicity nature, as opposed to the Morse oscillator, whose anharmonic character increases as the number of its finite states goes down, whereas that of Kratzer has no adjustable anharmonicity parameter. One can appreciate this by examining the force constants (curvature) of the two oscillators: the Morse oscillator curvature is dependent on its width parameter (bond strength), whereas the Kratzer curvature lacks any width-related parameter and, hence, is independent of it (leading to an infinite number of bound states) and, thus, is dependent only on frequency. As such, as much as the Kratzer and Morse oscillators eigenfunctions resemble each other, the above-cited differences will render slightly different spectra and dynamics, as will be discussed in the following sections.

Close examination of the hydrogen atom stationary states shows that not only these states,

$$R_{n\ell}(\zeta) = M_{n\ell}\zeta^{\ell} \exp\left(-\frac{\zeta}{2}\right) L_{n+\ell}^{2\ell+1}(\zeta)$$

$$= M_{n\ell}\zeta^{\ell} \exp\left(-\frac{\zeta}{2}\right) {}_1F_1\left(\begin{matrix}-(n+\ell) \\ 2(\ell+1)\end{matrix}\middle| \zeta\right) \tag{11}$$

resemble those of Kratzer and Morse but also the energies of these states can be recovered from the Kratzer oscillator eigenenergies, as well-elucidated in ref 18. $M_{n\ell}$ in eq 11 is a normalization constant that has no relevance here.

IV. ANHARMONIC LINEAR SPECTROSCOPY VIA KRATZER POTENTIAL

Suppose a quantum system is excited from an electronic ground state $|g\rangle$ to an excited state $|e\rangle$. The adiabatic electronic Hamiltonian of the system is

$$\hat{H} = H_g|g\rangle\langle g| + H_e|e\rangle\langle e| \tag{12}$$

where the nuclear Hamiltonians are

$$H_g = \sum_{j=1}^{\infty} \frac{P_j^2}{2\mu_j} + D_{ej}'' \left[\left(\frac{1}{q_j''}\right)^2 - 2\frac{1}{q_j''}\right] \tag{12a}$$

and

$$H_e = \sum_{j=1}^{\infty} \frac{P_j^2}{2\mu_j} + D_{ej}' \left[\left(\frac{1}{q_j'}\right)^2 - 2\frac{1}{q_j'}\right] \tag{12b}$$

Henceforth, the formal theory will be carried out over one mode, without any loss of generality, where confusion is unlikely to arise. Here, we follow the conventional notation in spectroscopy whereby the initial state is denoted by double-primed quantities, whereas the final state is denoted by single-primed ones. The linear dipole moment time correlation function (DMTCF) is given by

$$J(t) = \frac{\mathrm{Tr}\left(\exp\left(i\hat{H}t/\hbar\right) d \exp\left(-i\hat{H}t/\hbar\right) d \exp\left(-\beta\hat{H}\right)\right)}{\mathrm{Tr}\left(d^2 \exp\left(-\beta\hat{H}\right)\right)} \tag{13}$$

where β is the inverse temperature, $\mathrm{Tr}(\cdot)$ denotes the trace over the entire system, and d is the electronic transition dipole moment operator:

$$d = d_{eg}|e\rangle\langle g| + d_{ge}|g\rangle\langle e| \tag{14}$$

While the nuclear transition dipole moment operator d_{eg}, under the Born−Oppenheimer approximation, is a matrix element in the electronic subspace, it acts as an operator in the nuclear subspace. Expanding eq 13 in the electronic

two-dimensional basis set, assuming the electronic adiabatic gap is much greater than kT and invoking the Condon approximation, yields

$$J(t) = \frac{\mathrm{Tr}_{\tilde{N}}\left(\exp\left(iH_g t/\hbar\right)\exp\left(-iH_e t/\hbar\right)\exp\left(-\beta H_g\right)\right)}{Q} \tag{15}$$

where the partition function Q is

$$Q = \mathrm{Tr}_{\tilde{N}}\left(\exp\left(-\beta H_g\right)\right) \tag{15a}$$

where $\mathrm{Tr}_{\tilde{N}}(\cdot)$ denotes the trace over the nuclear degrees of freedom. In light of the above, one can assume that the equilibrium density operator of the entire system is

$$\rho = \frac{\exp\left(-\beta H_g\right)|g\rangle\langle g|}{Q} \tag{16}$$

That is, the entire system is in thermal equilibrium with the electronic ground state. Once the DMTCF is determined, the linear electronic absorption lineshape function may be calculated using

$$I(\omega) = \frac{1}{2\pi}\int_{-\infty}^{\infty} \mathrm{d}t J(t)\exp(i\omega t) \tag{17}$$

In the foregoing sections, one-mode excitation is assumed, while the rest of the modes remain in the ground state, and a similarity of normal coordinates in the ground and excited electronic states is assumed.

While the eigenfunctions of H_g, for one mode, are given as

$$\Psi''_n(q'') = A''_n q''^{\lambda''}\exp\left(-\eta''_n q''\right){}_1F_1\left(\begin{matrix}-n\\2\lambda''\end{matrix}\middle|2\eta''_n q''\right) \tag{18}$$

and those of H_e are given as

$$\Psi'_m(q') = A'_m q'^{\lambda'}\exp\left(-\eta'_m q'\right){}_1F_1\left(\begin{matrix}-m\\2\lambda'\end{matrix}\middle|2\eta'_m q'\right) \tag{19}$$

The ground-state quantities are

$$\lambda'' = \frac{1}{2} + \sqrt{\Omega''^2 + \frac{1}{4}} \tag{20a}$$

$$\eta''_n 2 = \frac{2\mu r''^2_e (D''_e - E''_n)}{\hbar^2} \tag{20b}$$

with $\Omega''^2 = 2\mu r''^2_e D''_e/\hbar^2$ and $q'' = r/r''_e$, whereas those of the excited state are

$$\lambda' = \frac{1}{2} + \sqrt{\Omega'^2 + \frac{1}{4}} \tag{20c}$$

$$\eta'_m 2 = \frac{2\mu r'^2_e (D'_e - E'_m)}{\hbar^2} \tag{20c}$$

with $\Omega'^2 = 2\mu r'^2_e D'_e/\hbar^2$ and $q' = r/r'_e$. Upon expanding the nuclear trace, in terms of anharmonic number states, and using trace invariance, $\{|\Psi''_n\rangle\}_{n=0}$, eq 15 reads

$$J(t) = Q^{-1}\sum_{n=0}^{\infty}\exp\left(-\beta E''_n\right)\exp\left(\frac{iE''_n t}{\hbar}\right)\langle\Psi''_n|\exp\left(-\frac{iH_e t}{\hbar}\right)|\Psi''_n\rangle \tag{21}$$

In order to proceed forward, one would need to surmount the dilemma of $\{|\Psi''_n\rangle\}_{n=0}$ not being eigenstates of $\exp(-iH_e t/\hbar)$. One may expand the ket $|\Psi''_n\rangle$, in terms of the eigenbasis set of the excited state nuclear Hamiltonian H_e, *vide supra*, which will involve some formidable integrals.

$$\langle r|\Psi''_n\rangle = \sum_{m=0}^{\infty} c_m\langle r|\Psi'_m\rangle \tag{22}$$

where the expansion coefficient c_{mn} is given by

$$c_{mn} = \int_0^{\infty}\Psi'_m{}^*(r)\Psi''_n(r)\,\mathrm{d}r \tag{23}$$

Equation 21 thus reads

$$J(t) = Q^{-1}\sum_{n=0}^{\infty}\exp\left(-\beta E''_n\right)\exp\left(\frac{iE''_n t}{\hbar}\right)\sum_{m=0}^{\infty}\exp\left(-\frac{iE'_m t}{\hbar}\right)|c_{mn}|^2 \tag{24}$$

$$c_{mn} = A''_n A'_m\int_0^{\infty}\left(\frac{r}{r''_e}\right)^{\lambda''}\left(\frac{r}{r'_e}\right)^{\lambda'}\exp[-\kappa r]{}_1F_1\left(\begin{matrix}-m\\2\lambda'\end{matrix}\middle|\alpha_2 r\right){}_1F_1\left(\begin{matrix}-n\\2\lambda''\end{matrix}\middle|\alpha_1 r\right)\mathrm{d}r \tag{24a}$$

where $\alpha_1 = 2\eta''_n/r''_e$, $\kappa = (\eta''_n/r''_e) + (\eta'_m/r'_e)$, $\alpha_2 = 2\eta'_m/r'_e$, and the partition function Q is given by

$$Q = \sum_{n=0}^{\infty}\exp\left(-\beta E_n\right) \tag{25}$$

Using the Landau and Liftshitz integral formula,[19,20]

$$\int_0^{\infty} x^{\alpha-1}\exp[-hx]{}_1F_1\left(\begin{matrix}a\\b\end{matrix}\middle|kx\right){}_1F_1\left(\begin{matrix}a'\\b'\end{matrix}\middle|k'x\right)\mathrm{d}x = h^{-\alpha}\Gamma(\alpha)F_2\left(\alpha; a, a'; b, b'; \frac{k}{h}, \frac{k'}{h}\right) \tag{26}$$

where $F_2(\cdot)$ is Appell's hypergeometric function,[21,27] which yields

$$c_{mn} = A''_n A'_m (r''_e)^{-\lambda''}(r'_e)^{-\lambda'}(\kappa)^{-(\lambda''+\lambda'+1)}\Gamma(\lambda''+\lambda'+1)\times F_2\left(\lambda''+\lambda'+1; -m, -n; 2\lambda', 2\lambda''; \frac{\alpha_2}{\kappa}, \frac{\alpha_1}{\kappa}\right) \tag{27}$$

$|c_{mn}|^2$ acts as a FCF for the corresponding anharmonic transition $m \leftarrow n$. Using eq 24 in eq 17 yields the homogeneous (single-site) absorption lineshape:

$$I(\omega) = \frac{\gamma Q^{-1}}{2\pi}\sum_{n=0}^{\infty}\sum_{m=0}^{\infty}\frac{|c_{mn}|^2\exp\left(-\beta E''_n\right)}{\left(\omega + E''_n - E'_m\right)^2 + (\gamma/2)^2} \tag{28}$$

dx.doi.org/10.1021/ct1007185 |J. Chem. Theory Comput. 2011, 7, 1804–1813

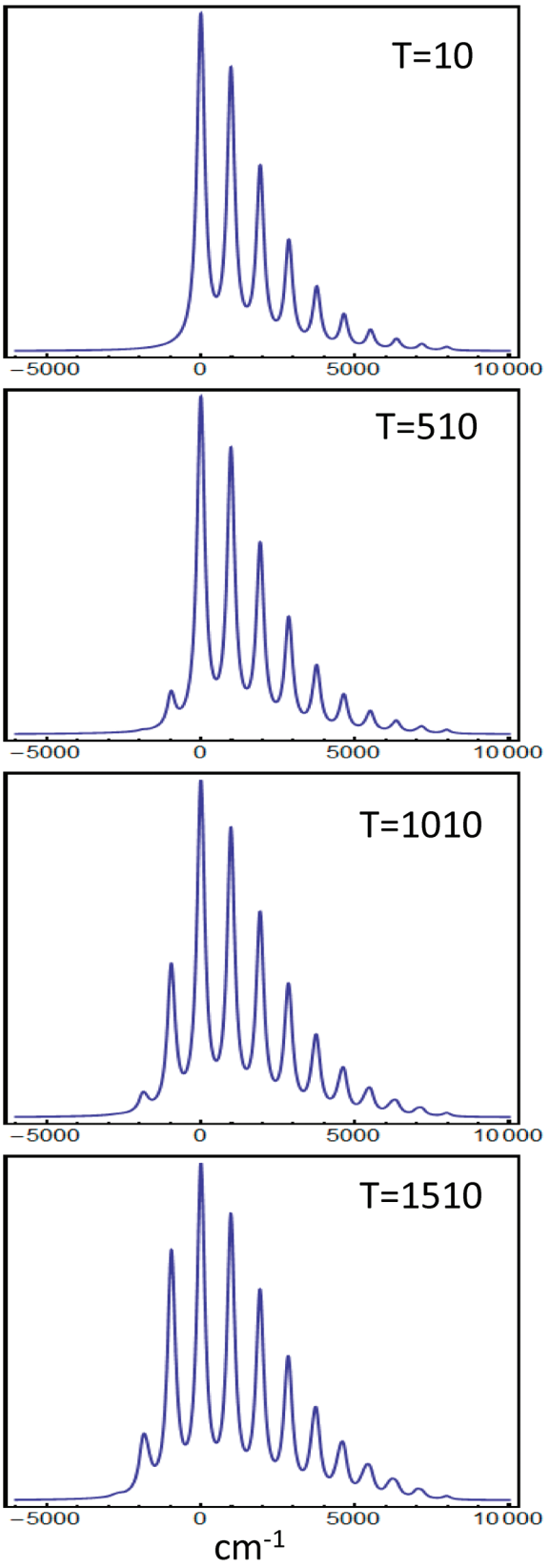

Figure 2. Linear homogeneous absorption spectra calculated with eqs 24−28, using $\omega'' = 1000\ \mathrm{cm}^{-1}$ and $r_e'' - r_e' = 1.5325$ at different temperatures. Note that the electronic bands appear at $\Delta E = E_m' - E_n'' = D_e'\{1 - (2\mu D_e' r_e'^2)/[\hbar^2(m + \lambda')^2]\} - D_e''\{1 - (2\mu D'' r_e''^2)/[\hbar^2(n + \lambda'')^2]\}$.

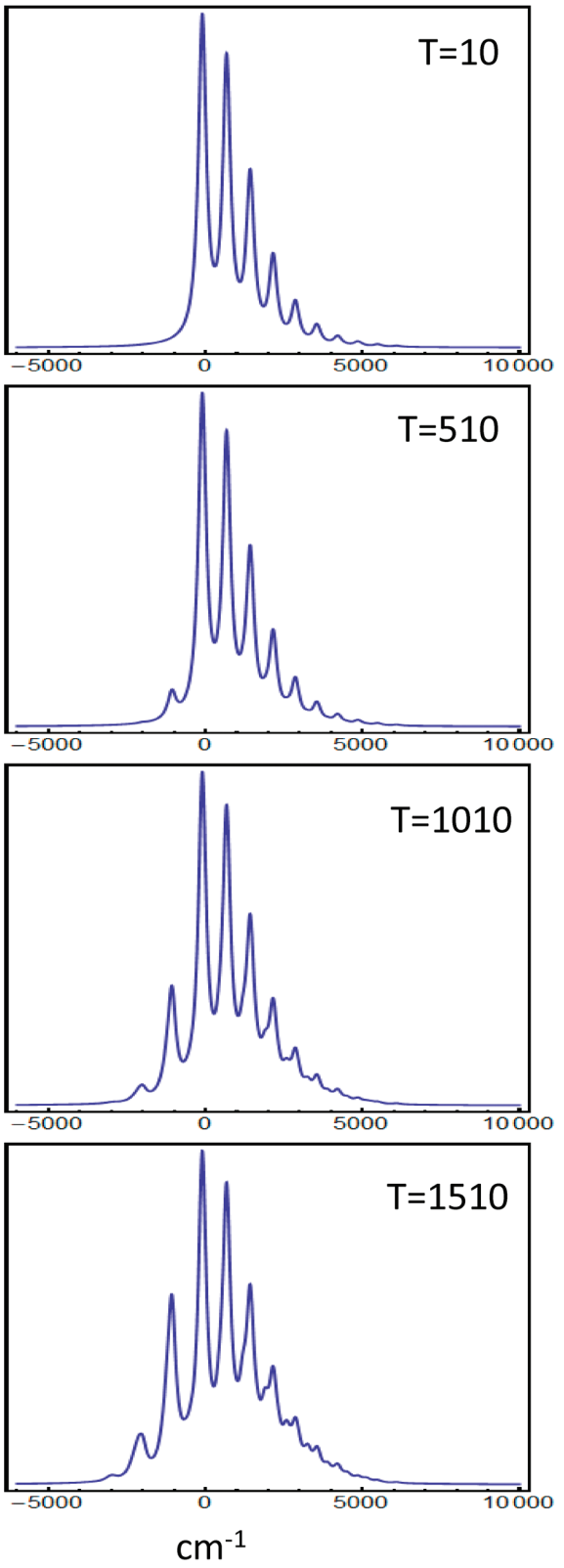

Figure 3. Linear homogeneous absorption spectra calculated with eqs 24−28 using $\omega'' = 1000\ \mathrm{cm}^{-1}$, $\omega' = 800\ \mathrm{cm}^{-1}$, and $r_e'' - r_e' = 1.5325$ at different temperatures.

where γ is the homogeneous line width. As well-elucidated in ref 3 and refs 28−30, eq 28 generates a lineshape of which all bands

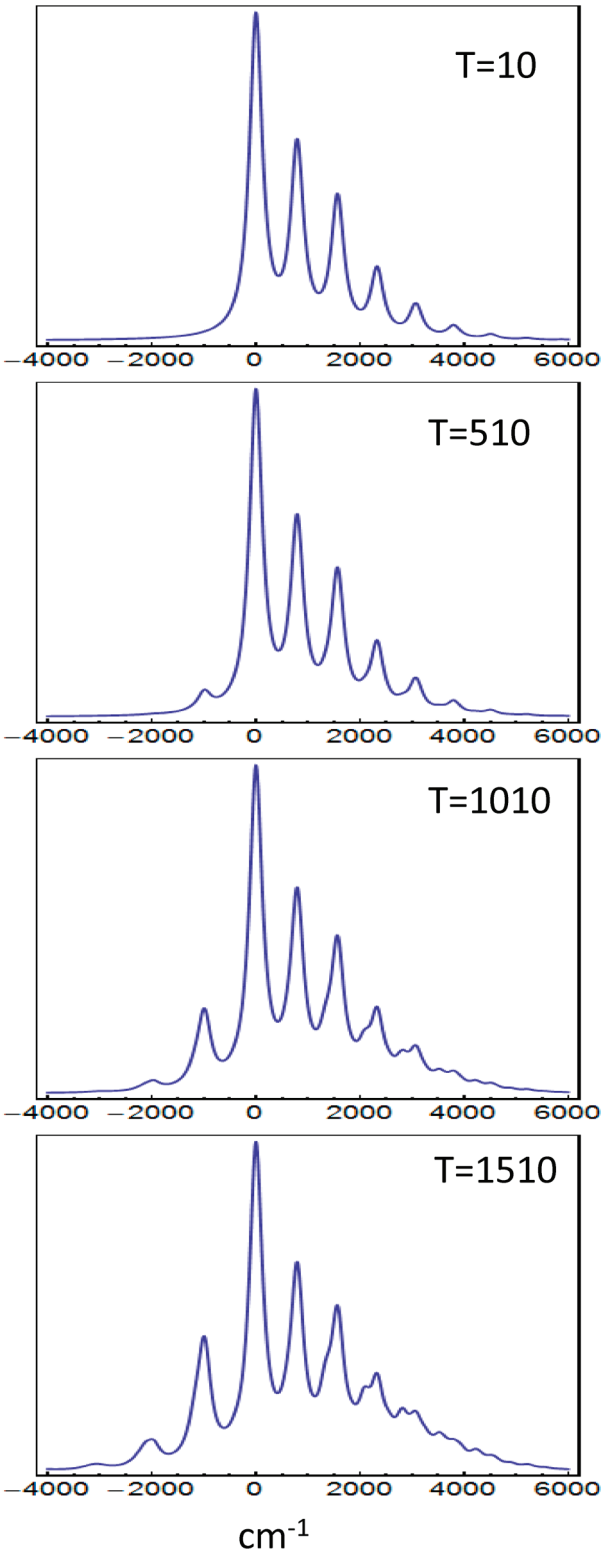

Figure 4. Linear homogeneous absorption spectra calculated, using the Morse oscillator DMTCF and the lineshape function developed in ref 2, with $\omega'' = 1000\ cm^{-1}$, $\omega' = 800\ cm^{-1}$, and $r_e'' - r_e' = 1.5325$ at different temperatures. Although this figure and Figure 3 are plotted on different wavenumber scales, one can easily see the similarity of the spectra calculated using the Kratzer and Morse oscillators.

have the same homogeneous width. For example, at low temperatures, one would find that the zero-phonon line (ZPL) and

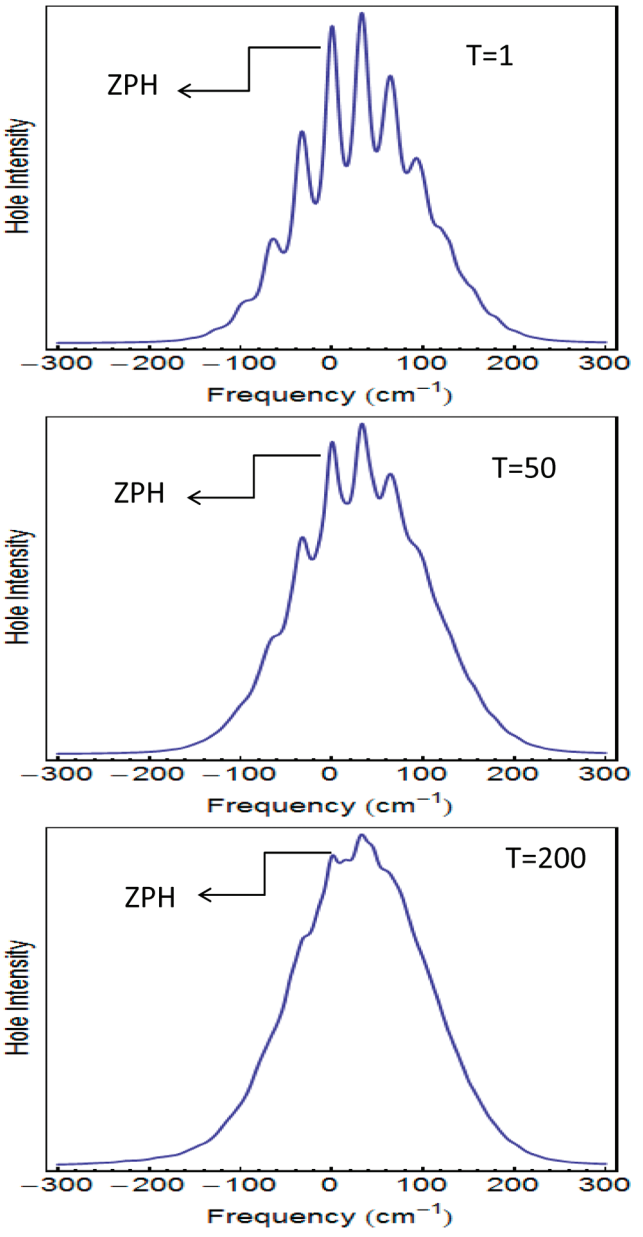

Figure 5. Hole-burned absorption lineshape with parameters of $\omega'' = 50\ cm^{-1}$, $\omega' = 40\ cm^{-1}$, $r_e' - r_e'' = 0.910$, $\omega_B = 0$, and $\Delta = 64.4\ cm^{-1}$ at different temperatures, showing the zero-phonon hole (ZPH) profile tapering off at higher temperatures. These calculations yield $\gamma_{ZPH} = 2\gamma_{el}$, as expected.

progression members have the same relaxation time constant, $1/\gamma$, which is unphysical.[3,28−30]

For an N-mode system, the total DMTCF can be expressed as follows, where the Duschinsky mixing effect is assumed to be negligible:

$$J(t) = \prod_{j=1}^{N} J_j(t) \qquad (29)$$

where $J_j(t)$ is the individual DMTCF for the jth mode provided in eq 24. In the case of exciting all the modes of this system, the absorption spectrum is then given by combining all of the

dx.doi.org/10.1021/ct1007185 |J. Chem. Theory Comput. 2011, 7, 1804–1813

individual mode spectra:

$$I(\omega) = \int d\omega_1 \int d\omega_2 \cdots \int d\omega_{N-1}\, I_1(\omega-\omega_1) I_2(\omega_1-\omega_2)\cdots I_N(\omega_{N-1}) \tag{30}$$

where $I_j(\omega)$ is the homogeneous absorption spectrum for mode j given by eq 28. To this end, one can identify the ZPL width, to probe the electronic pure dephasing, as illustrated in the next section.

A direct application of utilizing herein the DMTCF $J(t)$ and the corresponding absorption lineshape in eqs 24 and 28 is shown in Figure 2. Figure 2 uses a typical vibrational frequency of diatomic molecules, e.g., $\omega'' = 1000\ cm^{-1}$, $r_e' - r_e'' = 1.5325$ (dimensionless unit). Figure 3 shows the same spectra but with a frequency change upon excitation (curvature change) to $\omega' = 800\ cm^{-1}$. Figure 4 shows the same spectra as those shown in Figure 3 but calculated using the Morse oscillator absorption lineshape.[2,3] Spectra in Figures 3 and 4, which have been calculated using the Kratzer and Morse oscillator models, are comparable, showing clear similarities with a light difference in the hot band $0 \leftarrow 1$ transition.

V. PURE DEPHASING AND LINEAR ABSORPTION SPECTRA

If the system of interest consists of several anharmonic modes, the total DMTCF reads

$$F(t) = J_{el}(t) J_{anh}(t) \tag{31}$$

$$J_{el}(t) = \exp\left[-\frac{\gamma_{el}|t|}{2}\right] \tag{31a}$$

$$J_{anh}(t) = \prod_j^N J_{anh,j}(t) \tag{31b}$$

where $J_{anh,j}(t)$ is given by

$$J_{anh,j}(t) = \frac{1}{Q}\left\{|c_{00}|^2 \exp\left[-\beta\left(D_e'' - \frac{2D_e''2r_e''2\mu}{\hbar^2\lambda_e''2}\right) + i\Xi t/\hbar\right] + \sum_{n=1}^{\infty}\sum_{m=1}^{\infty}|c_{mn}|^2 \exp\left[-\beta E_n'' + \frac{it(E_n''-E_m')}{\hbar} - \frac{\gamma_j|t|}{2}\right]\right\} \tag{31c}$$

where

$$\Xi = D_e'' - D_e' + \frac{2D_e'2r_e'2\mu}{\hbar^2\lambda_e'^2} - \frac{2D_e''2r_e''2\mu}{\hbar^2\lambda_e''^2} \tag{31d}$$

The set of equations presetned as in eq 31 will lead to an electronic dephasing time equal to $1/\gamma_{el}$ and a vibrational relaxation time equal to $(\gamma_{el} + \gamma_j)^{-1}$. Of course, the dependence of γ_{el} on temperature is determined by the nature of the ensuing dephasing mechanism dictated by the guest−host relationship.[3,28−30] If one was to look *only* at the 0−0 transition (ZPL) rendered by eq 31c (before multiplying it by $J_{el}(t)$), it will have a delta function-like profile with a zero width and an intensity equal to

$$Q^{-1}|c_{00}|^2 \exp\left[-\beta\left(D_e'' - \frac{2D_e''2r_e''2\mu}{\hbar^2\lambda_e''^2}\right)\right] \tag{32}$$

where the overlap integral,

$$c_{00} = \frac{2^{\lambda''+\lambda'}(r'')^{-\lambda''}(r')^{-\lambda'}\Gamma(1+\lambda''+\lambda')\sigma'^{\lambda'+(1/2)}\sigma''^{\lambda''+(1/2)}\left(\frac{\sigma''}{r''}+\frac{\sigma'}{r'}\right)^{-(1+\lambda''+\lambda')}}{\sqrt{\lambda''\lambda' r'' r' \Gamma(2\lambda'')\Gamma(2\lambda')}} \tag{32a}$$

results from integrating the product of the vibronic ground-state wave functions, with

$$\sigma'' = \sqrt{\frac{2\mu r_e''2(D_e''-E_0'')}{\hbar^2}} \tag{32b}$$

$$\sigma' = \sqrt{\frac{2\mu r_e'2(D_e'-E_0')}{\hbar^2}} \tag{32c}$$

The above description is very similar to the treatment of the Morse oscillator dephasing problem given in ref 3. Fourier transforming equations 31 and 32 will produce absorption spectra in which the ZPL has zero width in the low-temperature limit and starts to gain some width as the temperature increases, causing the ZPL to broaden and eventually diminish in the high-temperature limit.

VI. ANHARMONIC HOLE-BURNING SPECTROSCOPY VIA THE KRATZER POTENTIAL

As elucidated in ref 3, although hole burning is a nonlinear technique, one may still calculate its lineshapes, using the linear correlation function $J(t)$, by calculating the absorption spectrum following a burn time η:

$$I_\eta(\omega,\omega_B) = \int_{-\infty}^{\infty} d\Omega \chi(\Omega-\nu_m) J(\omega-\Omega)\exp[-\theta J(\omega_B-\Omega)\eta] \tag{33}$$

where Ω is the variable frequency of the ZPL of a single absorber and ω_B is the burn frequency. The absorption spectrum before burning is $I_0(\omega)$, which is obtained by setting the burning time as $\eta = 0$. Thus, the hole-burned spectrum is given by

$$S_{HB}(\omega,\omega_B) = I_\eta(\omega) - I_0(\omega) \tag{34}$$

$\chi(\Omega-\nu_m)$ is a Gaussian function, with variance Δ^2 centered at ν_m, which governs the distribution of ZPL frequencies, because of structural heterogeneity. θ is the product of three terms: the

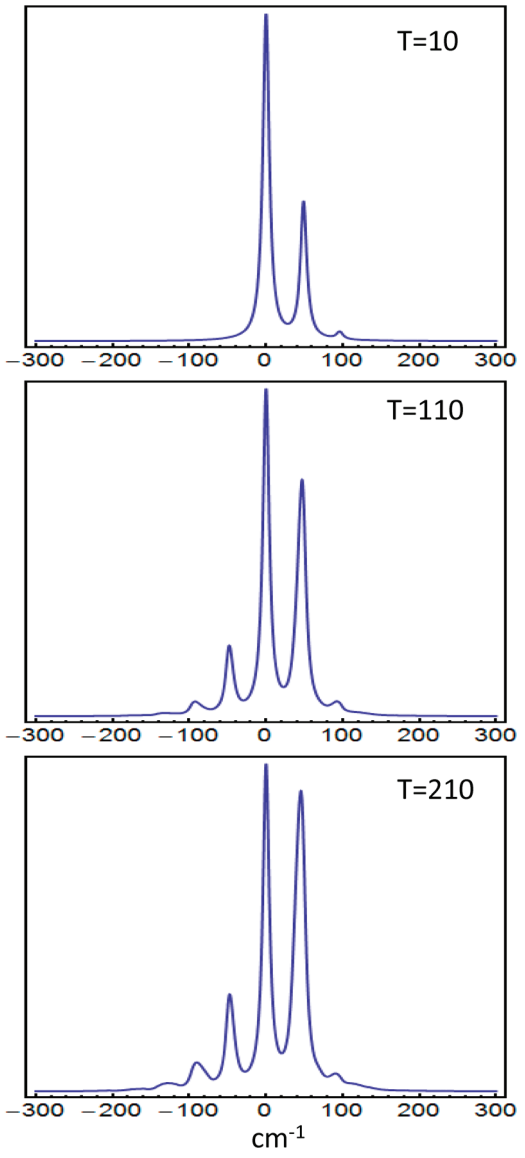

Figure 6. Linear homogeneous absorption spectra calculated using the Morse oscillator model with $\chi'' = 0.02$, $\omega'' = 50\ cm^{-1}$, $\chi' = 0.01$, $\omega' = 50\ cm^{-1}$, and $r_e' - r_e'' = 0.910$.

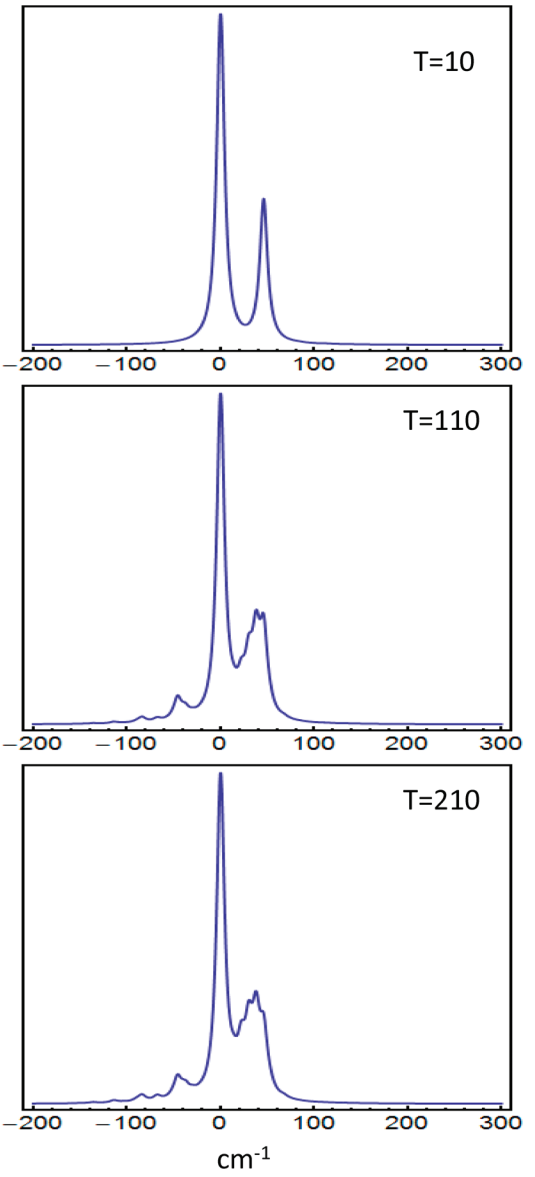

Figure 7. Same as in Figure 6, but with much higher anharmonicity (and, hence, much less vibrational bound states), to contrast the resulting spectra with those in Figure 6; see text for details.

absorption cross section, the laser burn flux, and the quantum yield for hole burning. Toutounji showed, using the theory of Bessel functions, that, in the case of a large inhomogeneous broadening, the hole-burning lineshape may be expressed in terms of the linear DMTCF:[3]

$$S_{HB}(\omega, \omega_B) = \frac{1}{2\pi}\theta\eta \int_{-\infty}^{+\infty} dt\,|J(t)|^2 \exp(-i\omega t)\exp(i\omega_B t) \tag{35}$$

The correctness and applicability of eq 35 was evidently ratified in ref 3. Figure 5 shows a model calculation of hole-burned absorption lineshapes with parameters of $\omega'' = 50\ cm^{-1}$, $\omega' = 40\ cm^{-1}$, $r_e' - r_e'' = 0.910$, and inhomogeneous broadening $\Delta = 64.4\ cm^{-1}$ at different temperatures, showing the zero-phonon hole (ZPH) and phonon-sideband hole in the burned spectra at $\omega_B = 0$. These parameters are similar to those used in ref 3 to simulate hole-burned spectra of APT in glassy ethanol.[31,32] In these spectra, the ZPH width is given as $\gamma_{ZPH} = 2\gamma_{el}$.

VII. CALCULATIONS AND DISCUSSION

Utilizing the Kratzer potential for modeling molecular vibrations can be fruitful, because the Morse and harmonic oscillators fail to reproduce the experimental vibrational ground-state energy ($2170.08\ cm^{-1}$) of the hydrogen molecule (H_2), whereas that of the Kratzer oscillator, using eq 3, successfully renders a value of $2170.12\ cm^{-1}$. (The Morse and harmonic oscillators yield values of 2201.6 and $2233.24\ cm^{-1}$ for the vibrational ground-state energy of H_2, respectively.)

Figure 6 shows different absorption spectra calculated at various temperatures using the Morse potential to describe the initial and final states. The parameters used in Figure 6 are close to those reported for CS_2 molecule in refs 7−9. Figure 6 was

dx.doi.org/10.1021/ct1007185 |J. Chem. Theory Comput. 2011, 7, 1804–1813

calculated with $\chi'' = 0.02$, $\omega'' = 50\ cm^{-1}$, $\chi' = 0.01$, $\omega' = 50\ cm^{-1}$, and $r'_e - r''_e = 0.910$. Figure 7, on the other hand, illustrates single-site absorption spectra with steep anharmonicity; it is calculated using values of $\chi'' = \chi' = 0.08$, $\omega'' = \omega' = 50\ cm^{-1}$, and $r'_e - r''_e = 0.910$ at the indicated temperatures. Figure 7 uses a largely anharmonic system with only six vibrational bound states in the upper and lower electronic states. Although the parameters in Figures 6 and 7 are the same, except for the anharmonicity constant, one can see how much of a critical role the potential anharmonicity may play in describing the spectra at hand. Although both figures were calculated using the Morse oscillator model, one can see how the disparity between the two sets of spectra starts to develop at higher temperatures, because of anharmonicity differences. Significant differences in the spectra in both figures are observed at high temperatures, and those differences are attributed to the differences in FCFs, which are governed by χ.[2]

It is worth noting, in light of Figures 6 and 7, that making a comparison between two Morse oscillators can sometimes be pointless, which is very unlike comparing two harmonic oscillators. This is because the number of bound states in a Morse potential is intimately dependent on the extent of its anharmonicity; for example, a largely anharmonic Morse oscillator can have as few as two bound states, whereas a Morse potential with a small anharmonicity (typically found to be ~0.02 in diatomics) can confine as many as 100 bound states. Comparing these two Morse oscillators would yield dissimilar results. Similarly, one must be cautious when comparing Kratzer and Morse oscillators. While the former has two parameters, namely, the bond length (r_e) and strength (D_e), the latter has r_e, D_e, and anharmonicity constants, which can influence the shape and, therefore, the spectral dynamics, of the Morse potential upon optical excitation. Thus, the anharmonicity constant may dramatically affect the lineshape, depending on its value. In contrast, the shape of the Kratzer potential does not vary upon excitation, because it lacks a potential width parameter (anharmonicity constant). However, under a carefully designed set of conditions, one may make the comparison.

VIII. CONCLUDING REMARKS

The motivation for this work is 2-fold: first, the report by Van Hooydonk[12] on the superiority of the Kratzer potential over the Morse potential in modeling ~300 diatomic molecules, and second, our calculation, which shows that the former potential gives much better vibrational ground-state energy for molecular hydrogen (H_2) than both Morse and harmonic oscillators (see section VII). The Kratzer oscillator features several advantages, which the Morse oscillator does not have, two of which are the ability to exactly solve the Schrodinger equation after including the centrifugal term, and the ability to obtain finite matrix elements in case of finite angular momenta, as noted in section I. It should be kept in mind that the Morse potential is a three-parameter potential, which will always have this "extra third parameter" as a merit over that of Kratzer, which will often make it outperform the Kratzer oscillator. However, as noted earlier, that extra parameter was not as helpful in calculating the vibrational ground-state energy of H_2: only the Kratzer oscillator can reasonably match its observed value in the laboratory, and not that of the Morse oscillator.

The dynamics of the Morse and Kratzer oscillators can be challenging under some conditions. Prezdho[14] and Cao[33] studied the dynamics of the Morse oscillator, where divergence problems arose. Therefore, as a maneuvering tactic, one may attempt to employ wavelets, because they have proven to be robust tools in treating divergence- and singularity-related problems. Also, it turns out that the Morse oscillator can readily be mapped onto the rotating Kratzer oscillator, as carried out by Stanek,[15] which, in turn, allows for the latter oscillator Wigner distribution function to be obtained.[34] This is important, because one can then work in phase space to probe mixed quantum-classical dynamics (MQCD), using an anharmonic Wigner distribution function, since MQCD formalism relies heavily on Wigner transforms and their properties for calculating cross- and autocorrelation functions in the mixed quantum-classical limit.[35−38]

In addition, Cooper[17] also presented a unified, and extremely useful, approach for utilizing Kratzer and Morse oscillators harmonically, using a combination of nonlinear coordinate transformation and similarity transformation. This transformation should allow for development of the time-Green's function of the Kratzer oscillator, whereby more efficient and accurate spectroscopy of complex systems may be probed. Finally, as an additional method to test the consistency with experiments, one may consider evaluating Franck−Condon factors (FCFs) upon making a transition from a Kratzer potential to that of Morse, to better suit the experimental conditions, *vide supra*, of the system of interest. However, the integrals that arise are challenging, because they tend to be of a two-center integral nature, and the best way to handle such a case is through the use of elliptical coordinates.

AUTHOR INFORMATION

Corresponding Author
E-mail: Mtoutounji@uaeu.ac.ae.

ACKNOWLEDGMENT

The author would like to thank Professors G. Van Hooydonk and M. Molski for useful discussions.

REFERENCES

(1) Toutounji, M. *Int. J. Quantum Chem.* **2010**, in press.
(2) Toutounji, M. *J. Phys. Chem. B* **2010**, DOI: 10.1021/jp104731s, and references therein.
(3) Toutounji, M. *J. Phys. Chem. C* **2010**, *114* (48), 20764−20774, and references therein.
(4) Moix, J. M.; Pollak, E. *J. Chem. Phys.* **2008**, *129*, 064515.
(5) Grad, J.; Yan, Y.; Mukamel, S. *J. Chem. Phys.* **1986**, *86*, 3441.
(6) Yan, Y.; Mukamel, S. *J. Chem. Phys.* **1988**, *88*, 5735.
(7) Tanimura, Y.; Ishaizaki, A. *Acc. Chem. Res.* **2009**, *42*, 1270and references therein.
(8) Suzuki, Y.; Tanimura, Y. *Phys. Rev. E* **1999**, *59*, 1475and references therein.
(9) Tanimura, Y.; Maruyama, Y. *J. Chem. Phys.* **1997**, *107*, 1779.
(10) Waldenstrom, S.; Razi, N. K. *J. Chem. Phys.* **1987**, *87*, 3563.
(11) Secrest, D. *J. Chem. Phys.* **1988**, *89*, 1017.
(12) Van Hooydonk, G. *Eur. J. Inorg. Chem.* **1999**, 1617.
(13) Wang, Z.; Heller, E. *J. Phys. A: Math. Theor.* **2009**, *42*, 285304.
(14) Heatwole, E. M.; Prezhdo, O. V. J. *Chem. Phys.* **2009**, *130*, 244111.
(15) Stanek, J. *Int. J. Quantum Chem.* **2009**, *110*, 1615.
(16) Molski, M. *Phys. Rev. A* **2007**, *76*, 022107.
(17) Cooper, I. *Chem. Phys.* **1988**, *121*, 343.
(18) Fernández, F. M.; Castro, E. A. Three-Dimensional Lie Algebras and Some of Their Realizations in Quantum Mechanics. Chapter 5

in *Algebraic Methods in Quantum Chemistry and Physics*; Klein, D., Randic, M., Eds.; CRC Press: Boca Raton, FL, 1996; p 71.
(19) Saad, N.; Hall, R.; Katabeh, D., Q. *J. Math. Phys.* **2005**, *46*, 022104.
(20) Saad, N.; Hall, R. *J. Phys. A: Math. Gen.* **2003**, *36*, 7771.
(21) Murley, J.; Saad, N. *Tables of the Appell Hypergeometric Functions F_2*; arXiv:0809.5203v1 [math-ph], 2008. (Accessible via the Internet at http://arxiv.org/abs/0809.5203v1.)
(22) Matamala, A. *Int. J. Quantum Chem.* **2002**, *89*, 129.
(23) Setare, M. R.; Karimi, E. *Phys. Scr.* **2007**, *75*, 90.
(24) Van Hooydonk, G. *Spectrochim. Acta, Part A* **2000**, *56*, 2273.
(25) Van Hooydonk, G. *Phys. Rev. Lett.* **2008**, *100*, 159301.
(26) Van Hooydonk, G. *Z. Naturforsch.* **2009**, *64a*, 801.
(27) Opps, S; Saad, N.; Srivastava, H., M. *J. Math. Anal. Appl.* **2005**, *302*, 180.
(28) Toutounji, M.; Small, G. J.; Mukamel, S. *J. Chem. Phys.* **1998**, *109*, 7949.
(29) Toutounji, M.; Small, G. J. *J. Chem. Phys.* **2002**, *117*, 3848.
(30) Hays, J.; Lyle, P. A.; Small, G. J. *J. Phys. Chem.* **1994**, *98*, 7337and references therein.
(31) Reinot, T.; Kim, W.-H.; Hayes, J. M.; Small, G. J. *J. Chem. Phys.* **1996**, *104*, 793.
(32) Reinot, T.; Kim, W.-H.; Hayes, J. M.; Small, G. J. *J. Chem. Phys.* **1997**, *106*, 457.
(33) Wu, J.; Cao, J. *J. Chem. Phys.* **2001**, *115*, 5381.
(34) Bund, G., W.; Tijero, M. C. *J.s Phys. A: Math. Gen.* **2004**, *37*, 3687.
(35) Toutounji, M.; Kapral, R. *Chem. Phys.* **2001**, *268*, 279.
(36) Toutounji, M. *Chem. Phys.* **2003**, *293*, 311.
(37) Toutounji, M. *J. Chem. Phys.* **2005**, *123*, 244102.
(38) Toutounji, M. *J. Chem. Phys.* **2006**, *125*, 194520.